Available online at www.sciencedirect.com
ScienceDirect
Ceramics International 37 (2011) 3469–3476
CERAMICS INTERNATIONAL
www.elsevier.com/locate/ceramint

The sintering characteristics of pure tetrapod ZnO nanopowders prepared by thermal evaporation deposition (TED)

Jun Wu [a,*], Taotao Li [a], Chao Wang [a], Bailin Zhu [a], Run Wu [a], Changsheng Xie [b]

[a] Hubei Province Key Laboratory of Ceramics and Refractories, Department of Materials and Metallurgy, Wuhan University of Science and Technology, 430081 Wuhan, PR China
[b] Department of Materials Science and Engineering, Huazhong University of Science and Technology, 430074 Wuhan, PR China

Received 7 January 2011; received in revised form 19 May 2011; accepted 6 June 2011
Available online 12 June 2011

Abstract

The sintering characteristics of pure tetrapod ZnO nanopowders prepared by thermal evaporation deposition (TED) were studied in this paper. The results imply that there exist large amounts of interstitial zinc in the grains and much adsorbed oxygen on the surface. Even though the sintering temperature is low to about 500 °C, the pure tetrapod ZnO nanopowders grow sharply and reach about 280 nm. Using the expression of $G^n - G_0^n = Kt\ \exp(-Q/RT)$, the results of the kinetic grain growth study show that the kinetic grain growth exponent n is about 2.2. As for the grain growth activation energy Q, it is found that when the sintering temperature is lower than 900 °C, the activation energy is about 57.1 kJ/mol, and consequently increases up to 147.9 kJ/mol at the temperature higher than 900 °C. The growth mechanisms are discussed.

Keywords: A. Sintering; Tetrapod ZnO nanopowders; Interstitial zinc; Surface adsorbed oxygen

1. Introduction

As a kind of raw materials for the electronic ceramics, particularly for the varistors [1], ZnO powders with some kinds of dopants usually undergo sintering so as to obtain the desired electrical properties. Consequentially, the sintering characteristics of ZnO are most important for the excellent electrical properties besides the sort and content of dopants. In order to reveal the sintering mechanisms and grain growth law as thoroughly as possible, and obtain the values of the activation energy for the grain growth, ZnO powders with omnigenous sizes and shapes have become the subject of intensive investigation in the past several decades. Several equations, such as $G^n - G_0^n = Kt\ \exp(-Q/RT)$, have been proposed to describe the sintering behavior and calculate the grain growth activation energy [2]. The sintering mechanisms are interpreted with grainboundary, surface, volume and lattice diffusion etc. [3]. The results reveal that the grain growth exponent n of pure ZnO can change from 3 to 6 [2], while the grain growth activation energy Q varies from about 12.5 kJ/mol [4] to 461 kJ/mol [2]. Whittemore and Varela pointed out that the great variation in activation energies might result from the difference in the experiments and the materials [4], such as the surface area of ZnO powders, excess surface oxygen and whether the ZnO powders suffered pressing or not etc. Erhart and Albe calculated the migration energy of zinc and claimed that the most mobile defects were zinc interstitials followed by oxygen interstitials, zinc vacancies, and oxygen vacancies, and self-diffusion occurred via vacancy mechanism under predominantly oxygen-rich and n-type conditions [5]. Binks also found that there exists close relationship among the migration energy, lattice direction and the type of zinc and oxygen, of which the activation energy of $Zn_i^{\bullet\bullet}$ migrated along C direction is the lowest one with 77 kJ/mol [6]. Tomlins et al. found that the activation energy of oxygen diffusion in single-crystal ZnO and that of zinc self-diffusion in needle shape ZnO were about 308.2–404.5 kJ/mol [7] and 372 kJ/mol [8] respectively.

Recently, the sintering characteristics of ZnO nanopowders attract much more attention and become the focus of investigation [9–17]. Ewsuk et al. found that the apparent activation energy of densification for the nano ZnO powders was 268 ± 25 kJ/mol [12]. Hynes et al. revealed that the grain growth activation energy of nanocrystalline ZnO grains was extremely low to about 20 kJ/mol but increased to 54 kJ/mol at

* Corresponding author.
E-mail addresses: wujun629@hotmail.com, woojun@tom.com (J. Wu).

0272-8842/$36.00
doi:10.1016/j.ceramint.2011.06.002

>500 °C, and reached 275 kJ/mol when the temperature was in the range of 600–700 °C [13]. Qin et al. found the grain growth activation energy for the nanocrystalline ZnO prepared through chemical route with 20 nm were 64 ± 6 kJ/mol in the temperature range of 973–1173 K [14]. As for the growth mechanisms, Groza et al. pointed out that being different from those with micrometer size, ZnO nanopowders were thermodynamically unstable due to large surface area and some other mechanisms, e.g., dislocation motion, grain rotation, viscous flow and grain boundary slip, were suggested to explain the sintering process [18].

It is worth noting that the preparation methods of the raw ZnO powders used in above mentioned researches are different, the preparation method will significantly influence the defect forms and the stoichiometric proportion between zinc and oxygen in ZnO. The tetrapod ZnO nanopowders prepared by thermal evaporation deposition (TED) may be quite different from the ZnO nanopowders prepared by other methods, especially the chemical route. As a result, their sintering characteristics were studied in this paper, and then the grain growth mechanisms were discussed.

2. Experimental procedure

The manufacture process of the tetrapod ZnO nanopowders prepared by TED was described in another article in detail [19]. In present work, before DSC thermoanalysis test, the as-prepared tetrapod ZnO nanopowders were baked at about 150 °C for 8 h in dry air so as to remove the surface adsorbed gas impurities as far as possible, and then were pressed to flakes at different pressures. Afterwards, a very small quantity of the flake was cut as a sample for DSC thermoanalysis test with model DSC 2010 thermal analyzer. The heating rate was 15 °C/min, the crucible was high purity Al_2O_3, and the gas media were pure O_2 and pure Ar, respectively.

After ball-milled for 8 h, the tetrapod ZnO nanopowders were pressed into discs of about 20 mm in diameter at a pressure of about 200 MPa, and then the green discs with a relative density of about 58–62% TD (TD = 5.645 g/cm^3) were obtained. A series of green discs were sintered in a temperature range of 500–1170 °C in air for 2 h in a conventional electric furnace and then cooled down to room temperature in air. The specimens of the other two series were isothermally sintered at 800 °C and 1000 °C respectively for five different times (0.5, 1, 1.5, 3 and 4 h). The morphologies and selected area electron diffraction (SAED) of the as-prepared tetrapod ZnO nanopowders were operated with Philips CM200 and its crystal structure was examined by X-ray diffractometer with Cu target (λ = 0.15406 nm). The morphologies and sizes of the sintered specimens were observed and measured with JEOL JSM-35A and FEI Nova400 Nano SEM, respectively.

3. Results and discussion

The morphologies of the as-prepared tetrapod ZnO nanopowders are shown in Fig. 1a. It can be found that every nanopowder has 4 needles, each of which is about 20–40 nm in diameter and 800–1000 nm in length, the SAED pattern of randomly selected single needle shows that each needle is a single crystal, as shown in Fig. 1b. The XRD results indicate that the as-prepared tetrapod ZnO nanopowders are of wurtzite structure (No. 36-1451 JCPDS card) and the average crystallite size calculated by Scherrer formula is about 44.7 nm, which is approximate to the value of the diameter of the needles estimated with TEM, as shown in Fig. 2a and b. Furthermore, no evidence can be found for the existence of pure zinc from the results of TEM, SAED and XRD.

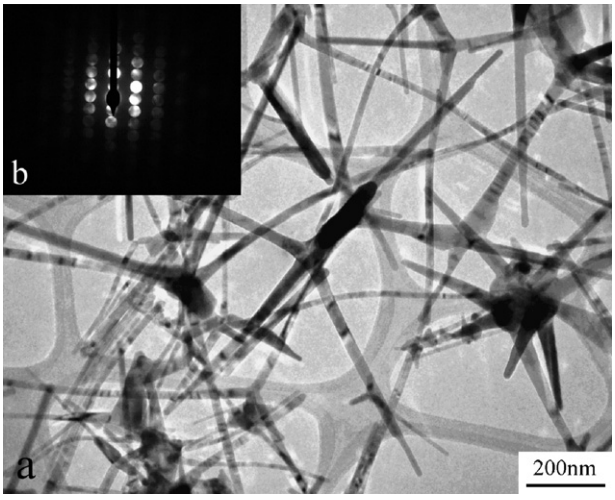

Fig. 1. (a) Morphologies of the as-prepared tetrapod ZnO nanopowders and (b) SAED pattern of a single needle.

The results of the DSC curves tested in pure Ar and pure O_2 respectively show that for all the samples, three endothermic peaks were observed, in which one shifted with the change of the gas type, the other two did not. It can also be found that the pressure did not influence the endothermic process, as shown in Fig. 3a–d. There is no doubt that the weak endothermic peak at 234–238 °C is related to the chemical desorption process of the adsorbed gas on the surface of the tetrapod ZnO nanopowders, even though they were baked at 150 °C for 8 h in dry air before

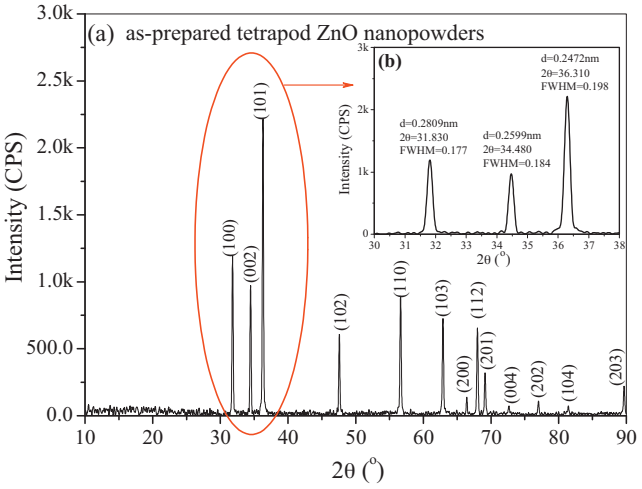

Fig. 2. XRD spectra of tetrapod ZnO nanopowders. (a) Range of 10–90° and (b) range of 30–38°.

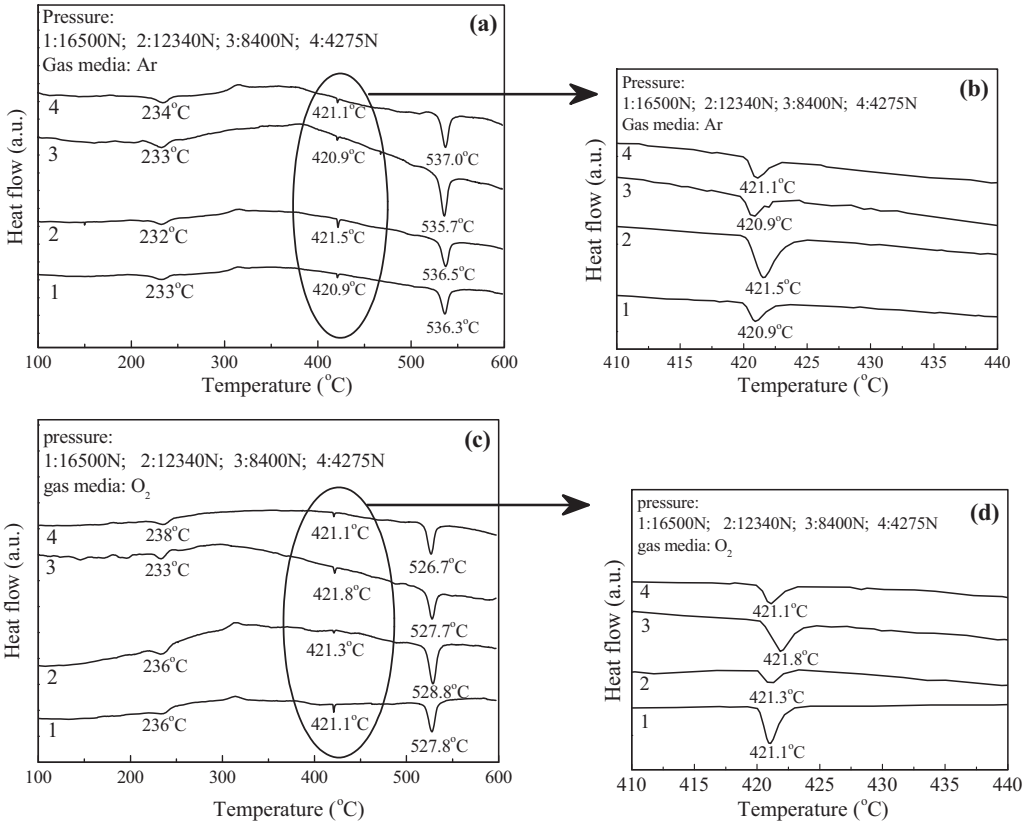

Fig. 3. DSC curves tested in different gas media. (a and b) in pure Ar and (c and d) in pure O_2.

test. It should be noted that there is a weak endothermic effect at about 421 °C, which is close to the melting point of pure zinc and did not shift with the change of the gas, as shown in Fig. 3b and d. This endothermic peak implies the possibility of the existence of pure zinc in the tetrapod ZnO nanopowders, but the results of XRD, TEM and SAED confirm no pure zinc exists. Since the tetrapod ZnO nanopowders were prepared under the condition of lack of oxygen, the stoichiometric proportion of zinc to oxygen is much larger than 1. Consequently, a possible explanation for the very weak endothermic peak at about 421 °C is that there exists much interstitial zinc and their diffusion behavior is similar to the melting process of zinc.

On the other hand, it needs to pay close attention to the third endothermic peak, which shifted from about 536 °C with the strength of 1.4–1.6 J/g in pure Ar to about 528 °C with that of 1.1–1.3 J/g in pure O_2. The results demonstrate that this endothermic process is related to the O_2 partial pressure, that is, the higher the O_2 partial pressure, the lower the temperature of the endothermic peak, and the lower the heat absorption capacity. This is in agreement with Gupta's conclusion that the activation energy for the diffusion of zinc in ZnO when sintered in pure O_2 was lower than that in air [20].

Generally speaking, during the sintering process, a reversible reaction [21] can take place as follows:

$$ZnO \rightleftharpoons Zn^{(g)} + \frac{1}{2}O_2{}^{(g)} \quad (1)$$

The reaction equation implies that increasing the O_2 partial pressure will restrain the endothermic decomposition reaction of ZnO, and the temperature needed in pure O_2 is higher than that in air. On the contrary, an exothermic synthetic reaction between zinc and oxygen can take place at the same time and increasing the O_2 partial pressure is advantageous to it. Dollimore and Spooner suggested that there was an excess of oxygen on the ZnO surface [3]. Castro and Aldao found that when the samples exposed to oxygen at the temperature of 300 °C after sintered at 600 °C, oxygen was adsorbed on the grains surface, and then diffused into the grains [22]. Jones et al. found that oxygen was adsorbed on ZnO surface as the form of $O_2{}^{2-}$ or O^- in the temperature range of 250–400 °C, then changed into O^{2-} when the temperature was higher than 450 °C and this process could continue to 550 °C, afterwards the O^{2-} would absorb heat and diffuse into the interior of ZnO [23]. In this work, because the tetrapod ZnO nanopowders own large specific surface area, there is much adsorbed, especially chemically adsorbed oxygen on the surface. During the heating process, the adsorbed oxygen may change into O^{2-} and diffuse into the interior of the ZnO grains, which is an endothermic process. Consequently, it can be concluded that a combination reaction between the interstitial zinc and the surface adsorbed oxygen can take place accompanied by their diffusion, and the endothermic peak at about 536 °C in pure Ar and about 528 °C in pure O_2 respectively, exactly confirms such diffusion and reaction process.

The SEM images of the samples sintered in a temperature range of 500–1170 °C in air for 2 h are shown in Fig. 4a–d. The results of the SEM images reveal that even though the specimens underwent sintering, they were porous and difficult

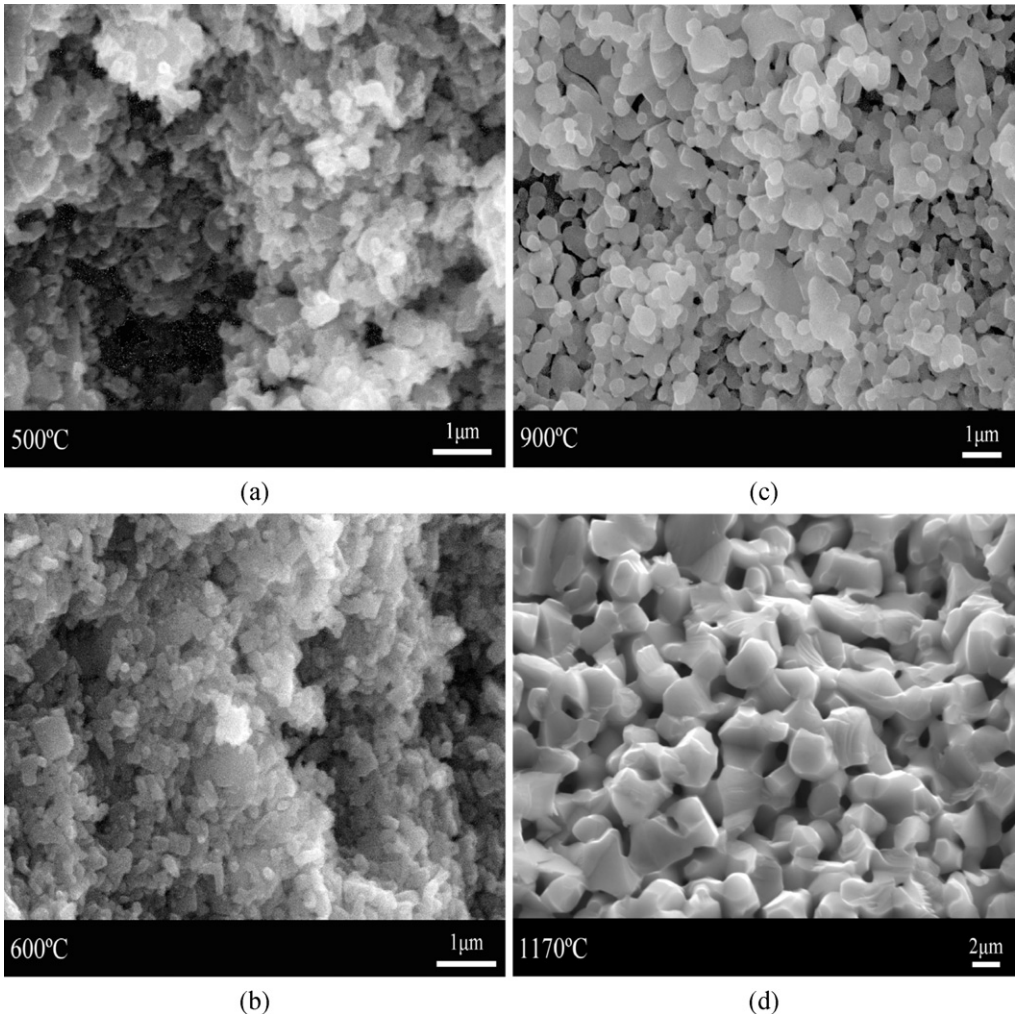

Fig. 4. SEM images of the samples sintered at different temperatures for 2 h. (a) 500 °C, (b) 600 °C, (c) 900 °C, and (d) 1170 °C.

to get high density with conventional sintering method. On the other hand, the ZnO nanopowders grew sharply and reached about 280 nm even though the sintering temperature was low to about 500 °C. Afterwards, the growth rate became slow in the temperature range of 500–900 °C. Whittemore and Varela [4] concluded that the mechanism for the initial sintering of ZnO from 450 °C to 700 °C in air was surface diffusion. Dollimore and Spooner [3] also pointed out that the initial excess surface adsorbed oxygen was depleted by the diffusion of zinc ions from the bulk to the surface during the sintering process. Such diffusion was very slow in the initial low-temperature sintering stage, and consequently the ZnO grain growth became slow.

When the temperature was higher than 900 °C, the grain growth became fast and reached about 4.06 μm after sintered at 1170 °C for 2 h. The average grain sizes of the ZnO grains are calculated by the formula as follows [2]:

$$\overline{G} = 1.56\overline{L} \tag{2}$$

where $\overline{L}$ is the average grain boundary intercept length of random lines measured by SEM.

The relationship between the sintering temperature and the grain sizes is shown in Fig. 5. Grain growth kinetics can be described by the phenomenological kinetic grain growth equation [2]:

$$G^n - G_0^n = K_0 t \ \exp\left(\frac{-Q}{RT}\right) \tag{3}$$

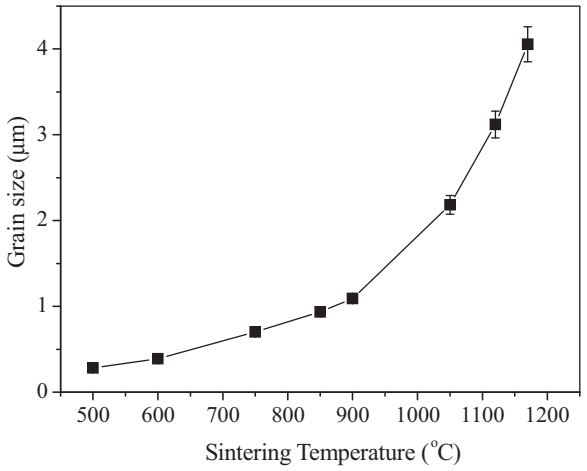

Fig. 5. The relation between the grain sizes and sintering temperature.

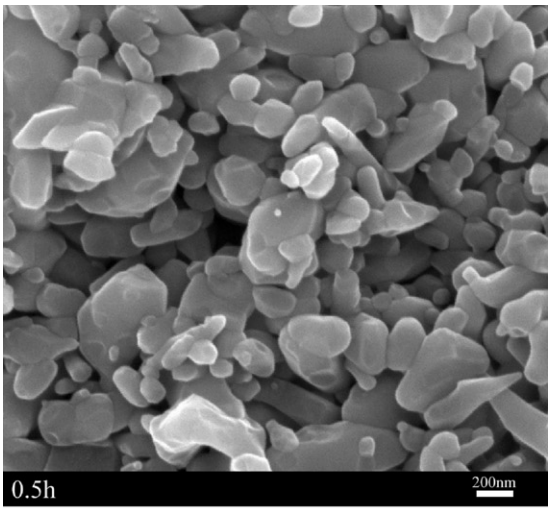

(a)

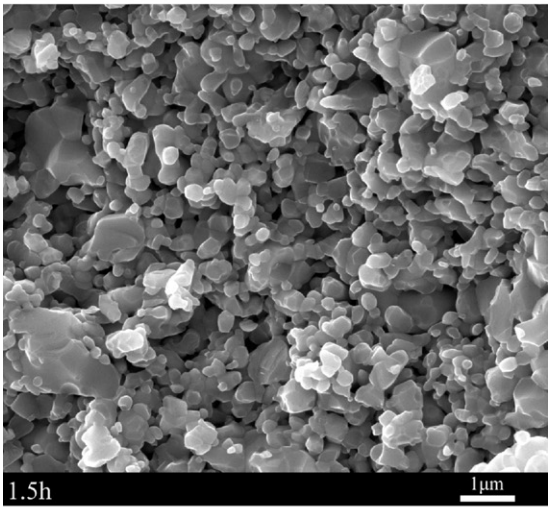

(b)

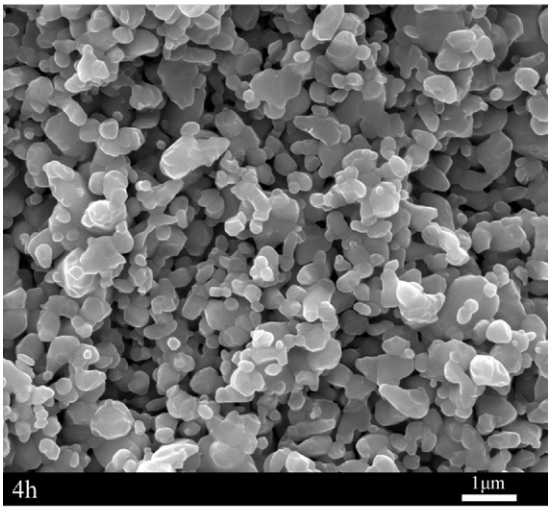

(c)

Fig. 6. SEM images of the samples sintered at 800 °C with different soaking time. (a) 0.5 h, (b) 1.5 h, and (c)4 h.

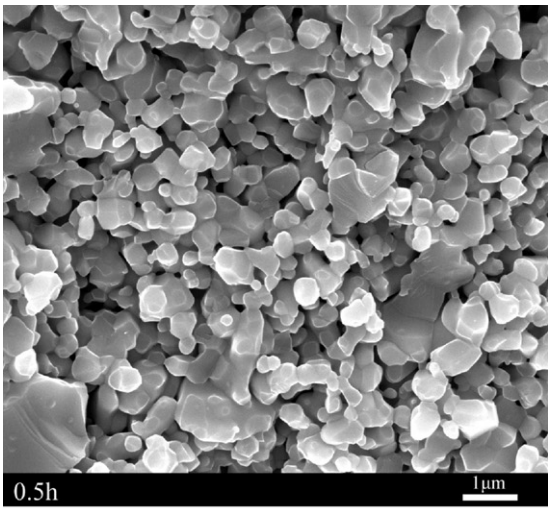

(a)

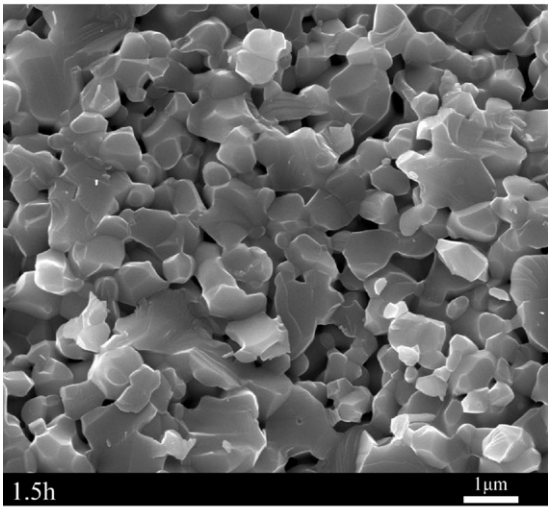

(b)

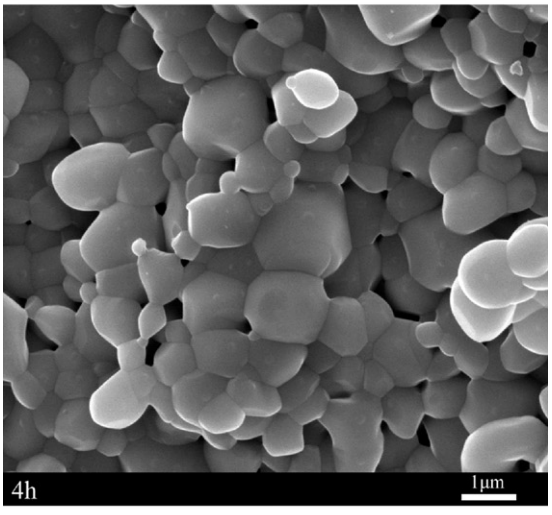

(c)

Fig. 7. SEM images of the samples sintered at 800 °C with different soaking time. (a) 0.5 h, (b) 1.5 h, and (c) 4 h.

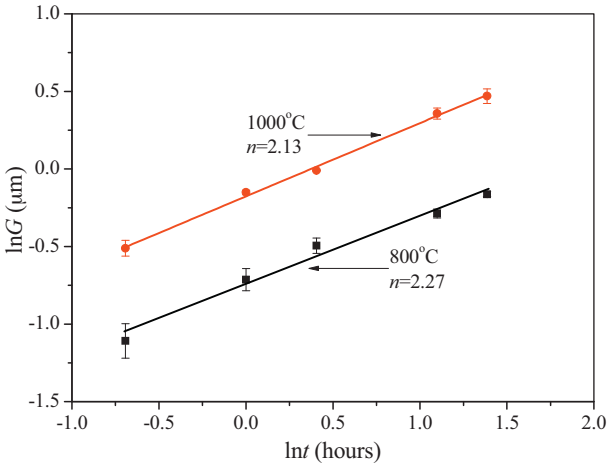

Fig. 8. The relationship between ln G and ln t and the calculated n.

Since G_0 is the initial grain size and is very small compared with the sintered ones and can usually be ignored. And then, formula (3) can be changed into the following form [2]:

$$\ln \frac{G^n}{t} = \ln K_0 - \frac{Q}{RT} \tag{4}$$

where G is the average grain size, n is the kinetic grain growth exponent, Q is the activation energy for the grain growth, R is the constant 8.31 J/kmol, K_0 is an exponential constant, and T is the absolute temperature.

The kinetic grain growth exponent n can be calculated from the isothermal grain size data when the equation is expressed as follows:

$$\ln G = \frac{1}{n} \ln t + \frac{1}{n}\left(\ln K_0 - \frac{Q}{RT}\right) \tag{5}$$

Finally, the reciprocal of the slope of the fitting line for ln G vs. ln t gives the n value. The SEM images for the isothermal sintering at 800 °C and 1000 °C respectively with different soaking time show that the grain grew generally with the increase of the sintering temperature and the prolongation of the soaking time, as shown in Figs. 6 and 7a–c respectively. The plots for ln G vs. ln t and the calculated n are shown in Fig. 8. The calculated n is about 2.13–2.27, and then the average value is about 2.2.

The plots for $\ln(G^{2.2}/t)$ vs. $1/T$ of the samples show that there conspicuously exist two kinds of different linear relationship between $\ln(G^{2.2}/t)$ and $1/T$, and 900 °C is a inflection point, which means that the activation energy Q and mechanism for the growth of this special ZnO nanopowders are different with the variation of sintering temperature range, as shown in Fig. 9. From the slope of the fitting line, the activation energy Q can be calculated, that is, Q_{LT} = 57.1 kJ/mol at the sintering temperature lower than 900 °C, and Q_{HT} = 147.9 kJ/mol at higher than 900 °C respectively.

The sintering mechanism and activation energy of ZnO grain growth are widely studied by many researchers and some results are summarized in Table 1. Being different from those of

Table 1
Summary of the kinetic grain growth exponent n, grain growth activation energy Q, initial grain size, manufacture method, sintering atmosphere, temperature range and grain growth mechanism of ZnO.

Ref.	Initial size	Manufacture method	Kinetic grain growth exponent n	Grain growth activation energy (kJ/mol)	Temperature range (°C)	Grain growth mechanism	Sintering atmosphere
[2]	0.1 μm	Oxidization of Zn vapor	3	224 ± 16	900–1400	Zn^+ lattice diffusion	In air
[4]	0.25 μm	Oxidization of Zn vapor	–	184	450–550	Surface diffusion	In air
[21]	–	–	3	253 ± 21	900–1100	Lattice diffusion of interstitial zinc atoms	In air
[24]	<0.2 μm	Decomposition of zinc carbonate	–	297.7	800–905	Volume diffusion and surface diffusion	In O_2 at 80 torr
[25]	<1 μm	–	3	212.7	950–1200		In air, O_2 and vacuum
[26]	0.1 μm	–	3	409	900–1100	Grain-boundary diffusion	In O_2
[27]	0.23 μm	–	–	210		Volume diffusion	
[13]	26–15 nm	–	3.5	20	<500	Rearrangement of the nanoparticle grains, surface and boundary diffusion, vapor transport	In air
				54	>500		
				275	600–700		
[14]	10–30 nm	Decomposition of $Zn_2CO_3(OH)_4{\cdot}H_2O$	4–7	64 ± 6	500–900		In air
[12]	48 nm	–	–	268 ± 25	950–1150	Grain boundary diffusion	In air
This work	20–40 nm in diameter and 800–1000 nm in length	Thermo evaporation deposition (TED)	2.2	57.1	<900	Diffusion and reaction of interstitial zinc and the surface adsorbed oxygen	In air
				147.9	>900	Vapor transport	

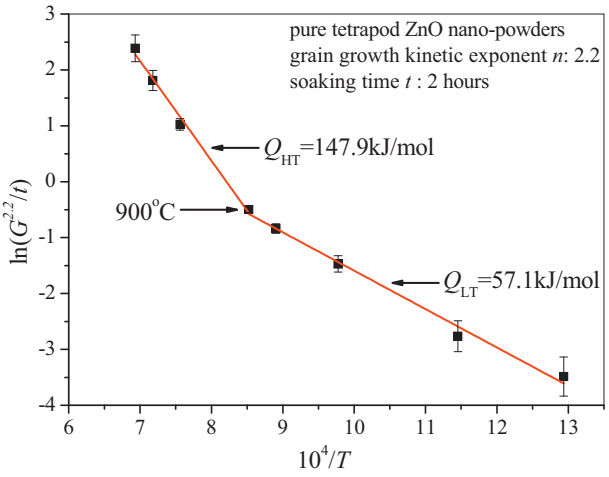

Fig. 9. $\ln(G^n/t)$–$10^4/T$ curve of the samples sintered at different temperatures.

the normal micro ZnO grains, Hynes et al. [13] revealed that the grain growth activation energy for the nanocrystalline ZnO grains was extremely low (just about 20 kJ/mol) and changed with the variation of sintering temperature range. Qin et al. [14] also found that the apparent activation energy for ZnO grain growth with 20 nm was 64 ± 6 kJ/mol in the temperature range of 973–1173 K. The important mechanisms of the nano ZnO growth were probably supposed to be rearrangement of the nanoparticle grains, surface and boundary diffusion, and vapor transport over 900 °C.

As for the tetrapod ZnO nanopowders prepared by TED, there exist much interstitial zinc and surface adsorbed oxygen. During the initial sintering stage of the temperature lower than 900 °C, the adsorbed oxygen was changed into O^{2-} and diffused into the ZnO grains, and simultaneous diffusion of the interstitial zinc also appeared. Consequently, an exothermic synthetic reaction between the interstitial zinc and the adsorbed oxygen appeared, and the activation energy is low to about 57.1 kJ/mol. After the depletion of interstitial zinc and the adsorbed oxygen, the above process is finished and the growth mechanism changes to common types, such as volume diffusion etc., and the activation energy for the grain growth rapidly increases to about 147.9 kJ/mol at the temperature higher than 900 °C. The activation energy estimated in this paper is near to those reported by other researchers, which means that the growth mechanisms may be similar.

4. Conclusions

The results of the kinetic grain growth study using the expression $G^n - G_0^n = Kt\ \exp(-Q/RT)$ show that the kinetic grain growth exponent n is about 2.2, and the activation energy Q changes with the variation of sintering temperature range. During the initial sintering stage of the temperature lower than 900 °C, the main mechanism for grain growth is a combination reaction between the interstitial zinc and the surface adsorbed oxygen accompanied by their diffusion, and the activation energy is low to about 57.1 kJ/mol. After the depletion of interstitial zinc and the adsorbed oxygen, the above process is finished and the growth mechanism changes to common types, such as volume diffusion etc., consequently the activation energy for the grain growth rapidly increases to about 147.9 kJ/mol at the temperature higher than 900 °C.

Acknowledgement

This work was financially supported by the National Nature Science Foundation of China (Grant No. 50902105) and Hubei Province Key Laboratory of Ceramics and Refractories. The authors sincerely thank Prof. S.L. Liu for the help in our English writing.

References

[1] M. Matsuoka, T. Masuyama, Y. Iida, Voltage nonlinearity of zinc oxide ceramics doped with alkali-earth metal oxide, Jpn. J. Appl. Phys. 8 (1969) 1275–1276.
[2] T. Senda, R.C. Bradt, Grain growth in sintering ZnO and ZnO–Bi_2O_3 ceramics, J. Am. Ceram. Soc. 73 (1990) 106–144.
[3] D. Dollimore, P. Spooner, Sintering studies on zinc oxide, Trans. Faraday Soc. 67 (1971) 2750–2759.
[4] O.J. Whittemore, J.A. Varela, Initial sintering of ZnO, J. Am. Ceram. Soc. 64 (1981) C-154–C-155.
[5] P. Erhart, K. Albe, Diffusion of zinc vacancies and interstitials in zinc oxide, Appl. Phys. Lett. 88 (2006) 201918.
[6] D.J. Binks, Ph.D thesis, University of Surrey, 1994.
[7] G.W. Tomlins, J.L. Routbort, T.O. Mason, Oxygen diffusion in single – crystal zinc oxide, J. Am. Ceram. Soc. 81 (1998) 869–876.
[8] G.W. Tomlins, J.L. Routbort, T.O. Mason, Zinc self-diffusion, electrical properties, and detect structure of undoped, single crystal zinc oxide, J. Appl. Phys. 87 (2000) 117–123.
[9] M. Mazaheri, A.M. Zahedi, S.K. Sadrnezhaad, Two-step sintering of nanocrystalline ZnO compacts: effect of temperature on densification and grain growth, J. Am. Ceram. Soc. 91 (2008) 1534–1538.
[10] T.K. Roy, D. Bhowmick, D. Sanyal, A. Chakrabarti, Sintering studies of nano-crystalline zinc oxide, Ceram. Int. 34 (2008) 81–87.
[11] L. Gao, Q. Li, W.L. Luan, H. Kawaoka, T. Sekino, K. Niihara, Preparation and electric properties of dense nanocrystalline zinc oxide ceramics, J. Am. Ceram. Soc. 85 (2002) 1016–1018.
[12] K.G. Ewsuk, D.T. Ellerby, Analysis of nanocrystalline and microcrystalline ZnO sintering using master sintering curves, J. Am. Ceram. Soc. 89 (2006) 2003–2009.
[13] A.P. Hynes, R.H. Doremus, R.W. Siegel, Sintering and characterization of nanophase zinc oxide, J. Am. Ceram. Soc. 85 (2002) 1979–1987.
[14] X.J. Qin, G.J. Shao, R.P. Liu, W.K. Wang, Sintering Characteristics of nanocrystalline ZnO, J. Mater. Sci. 40 (2005) 4943–4946.
[15] K.F. Cai, X.R. He, L.C. Zhang, Fabrication, properties and sintering of ZnO nanopowder, Mater. Lett. 62 (2008) 1223–1225.
[16] N. Hongsith, T. Chairuangsri, T. Phaechamud, S. Choopun, Growth kinetic and characterization of tetrapod ZnO nanostructures, Solid State Commun. 149 (2009) 1184–1187.
[17] M. Mazaheri, S.A. Hassanzadeh-Tabrizi, S.K. Sadrnezhaad, Hot pressing of nanocrystalline zinc oxide compacts: densification and grain growth during sintering, Ceram. Int. 35 (2009) 991–995.
[18] J.R. Groza, Nanosintering, NanoStmchmd Mater. 12 (1999) 987–992.
[19] R. Wu, C.S. Xie, Formation of tetrapod ZnO nanowhiskers and its optical properties, Mater. Res. Bull. 39 (2004) 637–645.
[20] T.K. Gupta, R.L. Coble, Sintering of ZnO: I densification and grain growth, J. Am. Ceram. Soc. 51 (1968) 521–525.
[21] S.D. Shin, C.S. Sone, J.H. Han, D.Y. Kim, Effect of sintering atmosphere on the densification and abnormal grain growth of ZnO, J. Am. Ceram. Soc. 79 (1996) 565–567.

[22] M.S. Castro, C.M. Aldao, Efects of the sintering temperature on the oxygen adsorption in ZnO ceramics, J. Eur. Ceram. Soc. 19 (1999) 511–515.
[23] A. Jones, T.A. Jones, B. Mann, J.G. Firth, The Effect of the physical form of the oxide on the conductivity changes produced by CH_4, CO and H_2O on ZnO, Sens. Actuators 5 (1984) 75–88.
[24] Y. Moriyoshi, W. Komatsu, Kinetics of initial sintering with grain growth, J. Am. Ceram. Soc. 53 (1970) 671–675.
[25] S.K. Dutta, R.M. Spriggs, Grain growth in fully dense ZnO, J. Am. Ceram. Soc. 53 (1970) 61–62.
[26] G.C. Nicholson, Grain growth in zinc oxide, J. Am. Ceram. Soc. 48 (1965) 214–215.
[27] J.P. Han, P.Q. Mantas, A.M.R. Senos, Sintering kinetics of undoped and Mn–doped zinc oxide in the intermediate stage, J. Am. Ceram. Soc. 88 (2005) 1326–1329.